

Effect of glass composition on the spectral and other properties of neodymium-doped borophosphate glasses

Shibin Jiang and Yasi Jiang

Shanghai Institute of Optics and Fine Mechanics, Academia Sinica, Shanghai (P. R. China)

Laser glasses of the system $R_2O(MO)-P_2O_5-B_2O_3-Ln_2O_3$ ($R = Li, Na, K; M = Ca, Sr, Ba; Ln_2O_3 = La_2O_3 + Nd_2O_3$) at high Nd^{3+} concentrations of $1 \cdot 10^{21}$ ions/cm³ were prepared. By using reactive atmosphere processing to remove hydroxyl groups, the infrared absorption coefficient at $3.5 \mu m$ due to OH^- groups was below $1 cm^{-1}$. Absorption and fluorescence spectra, fluorescence lifetimes and thermal expansion coefficients were measured, and the stimulated emission cross-section for the ${}^4F_{3/2} - {}^4I_{11/2}$ transition and the quantum efficiency were calculated.

The results indicate that the borophosphate glass is possessed of a large stimulated emission cross-section, especially for alkali oxide containing borophosphate glass systems in which the stimulated emission cross-section is larger than $4.4 \cdot 10^{-20} cm^2$, and the effect of alkali and alkaline earth ions depends on the bonding strength between the cation and oxygen. The influence of B_2O_3 in borophosphate glasses on the fluorescence lifetime is much less than that in silicate glasses, and the quantum efficiency of borophosphate glasses, different from borate and borosilicate glasses, is high. The introduction of B_2O_3 strengthens the structure resulting in a lower thermal expansion coefficient and an excellent thermal shock resistance.

Einfluß der Glaszusammensetzung auf die spektralen und andere Eigenschaften von neodym-dotierten Borophosphatgläsern

Es wurden Lasergläser des Systems $R_2O(MO)-P_2O_5-B_2O_3-Ln_2O_3$ ($R = Li, Na, K; M = Ca, Sr, Ba; Ln_2O_3 = La_2O_3 + Nd_2O_3$) mit hohen Nd^{3+} -Konzentrationen von $1 \cdot 10^{21}$ Ionen/cm³ hergestellt. Bei Anwendung eines Verfahrens mit reaktionsfähiger Atmosphäre zur Entfernung von Hydroxylgruppen lag der Infrarotabsorptionskoeffizient infolge des Auftretens von OH^- -Gruppen unter $1 cm^{-1}$. Die Absorptions- und Fluoreszenzspektren, die Fluoreszenzlebensdauer und der Wärmeausdehnungskoeffizient wurden gemessen, der Querschnitt der angeregten Emission für den ${}^4F_{3/2} - {}^4I_{11/2}$ -Übergang und die Fluoreszenzausbeute wurden berechnet.

Die Ergebnisse zeigen, daß Borophosphatgläser über einen großen Querschnitt der angeregten Emission verfügen, insbesondere trifft dies auf Alkalioxid enthaltende Borophosphatgläser zu, in denen dieser größer als $4,4 \cdot 10^{-20} cm^2$ ist. Der Einfluß von Alkali- und Erdalkalitionen hängt von der Bindungsstärke zwischen Kation und Sauerstoff ab. Die Fluoreszenzlebensdauer wird in Borophosphatgläsern von B_2O_3 weniger beeinflusst als in Silicatgläsern, die Fluoreszenzausbeute dagegen ist hoch, im Gegensatz zu der in Borat- und Borosilicatgläsern. Die Einführung von B_2O_3 festigt die Struktur, was zu einem niedrigen Wärmeausdehnungskoeffizienten und einer hohen Temperaturwechselbeständigkeit führt.

1. Introduction

Inertial confinement fusion research has made great progress in recent years [1 to 3]. High-power glass laser facility, one of the main fusion driver candidates, and slab glass lasers developing rapidly require an active medium with excellent laser performance and good thermomechanical properties in order to increase the power and repetition rate. Glass lasers used for material processing also require high thermal shock resistance to raise the repetitive rate. Several types of new laser glasses with improved thermal shock resistance and low-concentration quenching including ultraphosphate, silicophosphate and aluminophosphate have been investigated to meet this requirement [4 to 8].

Because the glass strength increases and the thermal expansion coefficient decreases by introducing B_2O_3 into phosphate glasses, borophosphate glasses might be a promising active medium with improved thermal shock resistance.

The useful spectral properties and the thermal expansion coefficient of borophosphate glasses are reported and discussed in this paper.

2. Experimental

All glasses were melted in a Siliconit furnace using fused silica crucibles. Compositions and the density, the refractive index, n_D , at $587.6 nm$, the Abbe number, ν , and the bonding strength between the cations $K^+, Na^+, Li^+, Ba^{2+}, Sr^{2+}, Ca^{2+}$ and oxygen, $F = 2z/a^2$, are given in table 1. The nonlinear refractive index coefficient, n_2 , calculated from equation (1) is included in table 1 [9].

$$n_2 = \frac{K' C (n_D^2 + 2)^2 (n_D - 1)}{\nu [1.5 + (n_D^2 + 2) (n_D + 1) \nu / (6 n_D)]^{1/2}} \quad (1)$$

where the empirical parameter $K' = 6.8 \cdot 10^{-20}$ in m^2/W and $C =$ velocity in m/s of light in vacuum. The Nd^{3+} concentration was maintained at $1 \cdot 10^{21}$ ions/cm³, and the sum of $La_2O_3 + Nd_2O_3$ was kept

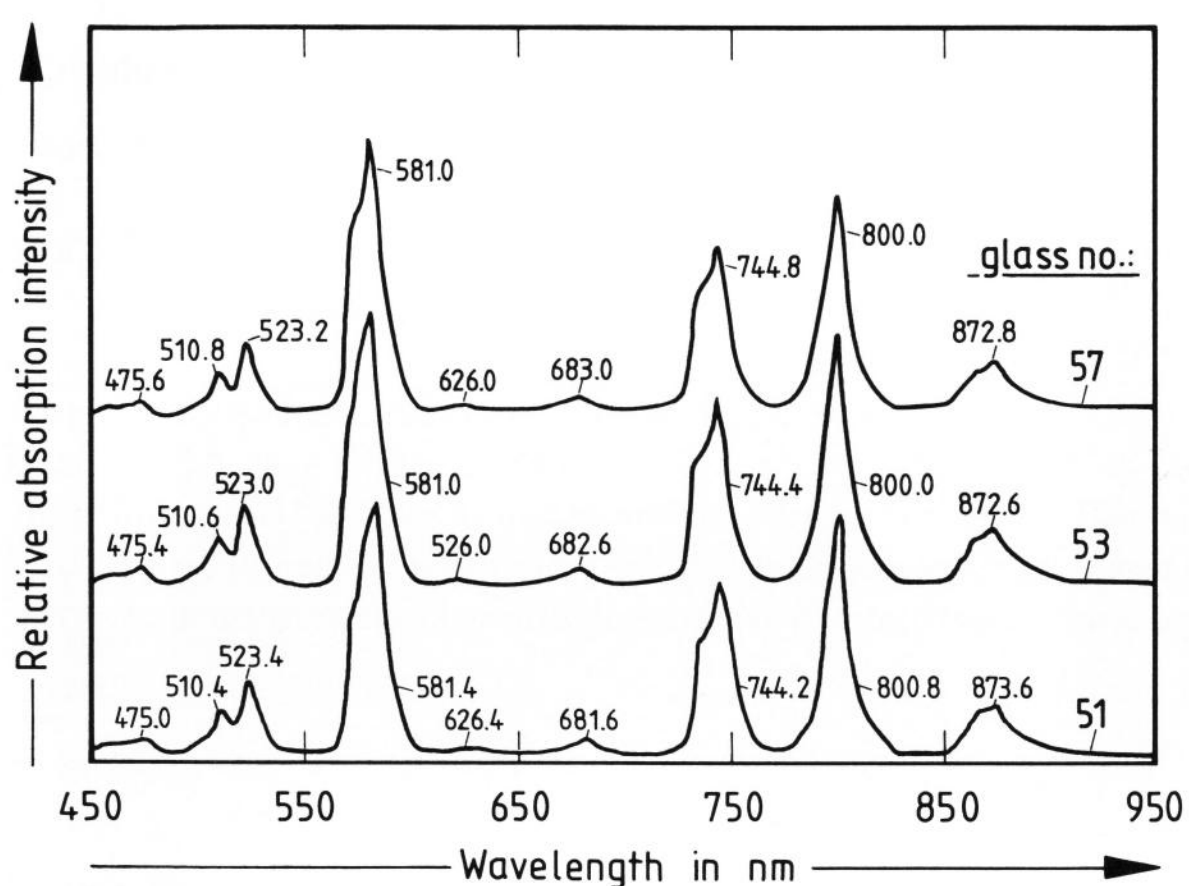
Received October 22, 1990.

Table 1. Compositions and physical properties of borophosphate glasses

glass no.:	50	51	52	53	54	55	56	57	58	59
compositions in mol%										
P ₂ O ₅	56	61	66	71	75	66	66	66	66	66
Ln ₂ O ₃ ¹⁾	6	6	6	6	6	6	6	6	6	6
B ₂ O ₃	0	5	10	15	19	10	10	10	10	10
K ₂ O	38	28	18	8	0					
Na ₂ O						18				
Li ₂ O							18			
BaO								18		
SrO									18	
CaO										18
properties										
concentration of Nd ³⁺ in 10 ²¹ /cm ³	1	1	1	1	1	1	1	1	1	1
density in g/cm ³	2.67	2.68	2.69	2.76	2.84	2.77	2.71	3.10	2.93	2.76
n ₂ in 10 ⁻¹³ esu	1.08	1.08	1.09	1.15	1.16	1.11	1.17	1.26	1.21	1.19
n _D	1.5102	1.5137	1.5241	1.5348	1.5367	1.5326	1.5388	1.5582	1.5461	1.5413
μ	65	66	67	66	66	67	66	65	65	65
F ²⁾	0.27	0.27	0.27	0.27	0.27	0.38	0.45	0.51	0.58	0.69

1) Ln₂O₃ = La₂O₃ + Nd₂O₃.

2) F corresponds twice to the field strength according to Dietzel.

Figure 1. Comparison of the absorption spectra of Nd³⁺ in three borophosphate glass samples no. 51, 53, and 57 (see table 1) at 298 K.

constant in order to minimize structural alteration in the glasses. High-purity raw materials were used to control the harmful transition metal content within the order of ppm. The infrared absorption coefficient at 3.5 μm caused by OH⁻ groups, which shortens the fluorescence lifetime of Nd³⁺, was maintained below 1 cm⁻¹ by using the Reactive Atmosphere Processing (RAP) to remove hydroxyl groups.

Absorption spectra from 450 to 950 nm were measured at room temperature using a spectrophotometer, fluorescence spectra in the 1.05 μm region were obtained using a monochromator, and the effective linewidth was determined, after calibrating the sensitivity of the detector, by integrating the fluorescence-line shape and dividing by the intensity at peak wavelength. Fluorescence lifetimes quoted are the first e-folding times in the decay curves and

the measurement uncertainty is estimated to be less than 10 μs. The stimulated emission cross-section for the ⁴F_{3/2} - ⁴I_{11/2} transition was calculated both by the Judd-Ofelt model developed by Krupke [10] and the modified Deutschbein formula [4], the accuracy is better than 10%. The fluorescence branching ratio, β, and the quantum efficiency were derived from the calculated Judd-Ofelt parameter. The glass transformation temperature, T_g, the softening temperature, T_f, and the thermal expansion coefficient, α, were measured by a dilatometer.

3. Results and discussion

3.1. Absorption spectra

Because the peak wavelength depends largely on the spectral energy level of the activator ion Nd³⁺, the absorption band peak wavelength of Nd³⁺ in borophosphate glasses changes only by a few in different glass matrixes. Three absorption spectra are presented in figure 1.

3.2. Effective linewidth and stimulated emission cross-section

The shift of fluorescence band peak wavelength of all specimens for the ⁴F_{3/2} - ⁴I_{11/2} transition, similar to the absorption peak wavelength, is small. The effective linewidth, Δλ_{eff}, for the 1.05 μm fluorescence band, the stimulated emission cross-section for the ⁴F_{3/2} - ⁴I_{11/2} transition calculated by the Judd-Ofelt model and the modified Deutschbein formula σ_{J-O}, σ_{Deut}, and the integrated absorption intensity of the 750 nm band, S_{750 nm}, are given in table 2.

Table 2. Spectral properties of borophosphate glasses

	glass no.									
	50	51	52	53	54	55	56	57	58	59
$\Delta\lambda_{\text{eff}}$ in nm	19.5	19.6	19.9	21.1	30.7	20.2	21.0	24.8	26.6	27.6
$S_{750\text{ nm}}$ in 10^{-20} cm^2	3.25	3.44	3.70	4.01	4.03	3.83	3.58	3.30	3.24	3.22
$\sigma_{\text{J-O}}$ in 10^{-20} cm^2	3.8	4.8	5.0	5.2	3.4	5.1	4.7	3.6	3.3	3.2
σ_{Deut} in 10^{-20} cm^2	3.7	4.5	4.8	4.9	3.4	4.8	4.4	3.5	3.4	3.2
Ω_2 in 10^{-20} cm^2	2.97	2.87	3.11	3.96	4.37	3.24	3.32	3.77	4.24	4.30
Ω_4/Ω_6	0.993	1.12	1.08	1.03	0.990	1.31	1.08	1.04	0.970	1.15
β	0.475	0.463	0.466	0.470	0.475	0.446	0.466	0.470	0.478	0.461
τ_f in μs	196	191	189	185	104	170	169	160	160	148
quantum efficiency	0.51	0.55	0.55	0.63	0.37	0.59	0.56	0.46	0.45	0.42

The effective linewidth widens with increasing B_2O_3 content or the bonding strength between cations and oxygen for both alkali and alkaline earth glass systems.

The stimulated emission cross-sections derived from the two methods are coincident. It can be taken from the modified Deutschbein formula that the stimulated emission cross-section depends on the refractive index, the integrated absorption intensity, S , of the 750 nm band and the effective linewidth of the 1.05 μm emission band. Although the effective linewidth widens with the introduction of B_2O_3 , the stimulated emission cross-section increases with increasing B_2O_3 content, different from the result of Kravchenko and Rudnitskii [11], because of the increase of the refractive index and the integrated absorption intensity of the 750 nm band for borophosphate glasses. A monotonic change of the stimulated emission cross-section occurs in the order K–Na–Li–Ba–Sr–Ca when the kind of network modifier was changed. Table 2 indicates that the borophosphate glass has a large stimulated emission cross-section, especially for alkali oxide glass systems in which the stimulated emission cross-section is larger than $4.4 \cdot 10^{-20}\text{ cm}^2$.

The Judd-Ofelt parameter, Ω_2 , the ratio of Ω_4/Ω_6 and the ${}^4\text{F}_{3/2} - {}^4\text{I}_{11/2}$ fluorescence branching ratio, β , were also presented in table 2. The parameter Ω_2 , the best indicator of differences in the local environment of Nd^{3+} in materials, increases with increasing B_2O_3 content and the bonding strength between cations and oxygen. Similar to the results of Weber et al. [12], the fluorescence branching ratio depends on the ratio Ω_4/Ω_6 although variations in the values of β with compositional changes are small.

3.3. Fluorescence lifetime and quantum efficiency

Similar to aluminophosphate glasses, the charge compensation of trivalent boron and pentavalent phosphorus in tetrahedral coordination occurs when introducing B_2O_3 into phosphate glass. The combination of a boron–oxygen tetrahedral unit (BO_4) and

a neighbouring phosphorus–oxygen tetrahedron (PO_4) would increase the number of bridging oxygens and weaken the interaction of the surrounding coordination polyhedra with the Nd^{3+} activator in borophosphate glasses. Thus, the influence of B_2O_3 on the fluorescence lifetime of the Nd^{3+} ion is much less than that in silicate glasses. The effect of boron, alkali and alkaline earth oxide on the fluorescence lifetime and quantum efficiency can be seen from table 2. It is shown that the variation of the fluorescence lifetime with the B_2O_3 content in borophosphate glasses is not significant, and the increase of the fluorescence lifetime with increasing bonding strength between cations and oxygen is not remarkable yet.

The nonradiative transition probability is so high that the quantum efficiency is very low for both borate and borosilicate glasses although the Einstein spontaneous emission coefficient is very large [13]. The low-quantum efficiency for borate and borosilicate glasses limits their practical application. The decrease of the interaction of the surrounding coordination polyhedra with the activator ions Nd^{3+} would reduce the nonradiative transition probability of Nd^{3+} in borophosphate glasses. It is demonstrated by the high-quantum efficiency of borophosphate glasses. Therefore, high-gain coefficients may be derived from neodymium borophosphate laser glasses. The borophosphate glass with large stimulated emission cross-section and high quantum efficiency might be a type of promising laser glass.

The interaction between pairs of Nd^{3+} ions brings about the concentration quenching of fluorescence when the Nd^{3+} ion concentration is above $2 \cdot 10^{20}$ ions/ cm^3 in most laser glasses. Figure 2 shows the concentration quenching curve for the glass $18\text{ K}_2\text{O} \cdot 10\text{ B}_2\text{O}_3 \cdot 6(\text{Nd}_2\text{O}_3 + \text{La}_2\text{O}_3) \cdot 66\text{ P}_2\text{O}_5$, and that of aluminophosphate glass is also shown for the sake of contrast [4]. Additional Nd_2O_3 was introduced when the sum of La_2O_3 and Nd_2O_3 exceeded 6 mol%. When the Nd^{3+} concentration is low, the fluorescence lifetime of borophosphate is smaller than that of aluminophosphate glass, for the field strength of boron is much larger than that of

Table 3. Thermal and thermomechanical properties of borophosphate glasses

	glass no.									
	50	51	52	53	54	55	56	57	58	59
T_g in °C	393	390	445	542	723	463	485	548	578	595
T_f in °C	409	427	497	597	758	500	524	587	611	637
$\alpha_{25/100}$ in K^{-1}	136	113	101	74	50	82	72	86	82	56
κ in $W/(m \cdot K)$	0.40	0.57	0.73	0.89	1.02	0.86	0.92	0.83	0.90	0.99
E in $10^{-5} N/cm^2$	36.3	46.1	56.9	67.7	77.5	59.8	72.6	64.7	66.7	71.6
μ	0.44	0.33	0.27	0.23	0.20	0.25	0.22	0.24	0.24	0.24
FOM'	0.45	0.71	0.92	1.35	2.07	1.28	1.35	1.11	1.24	1.85

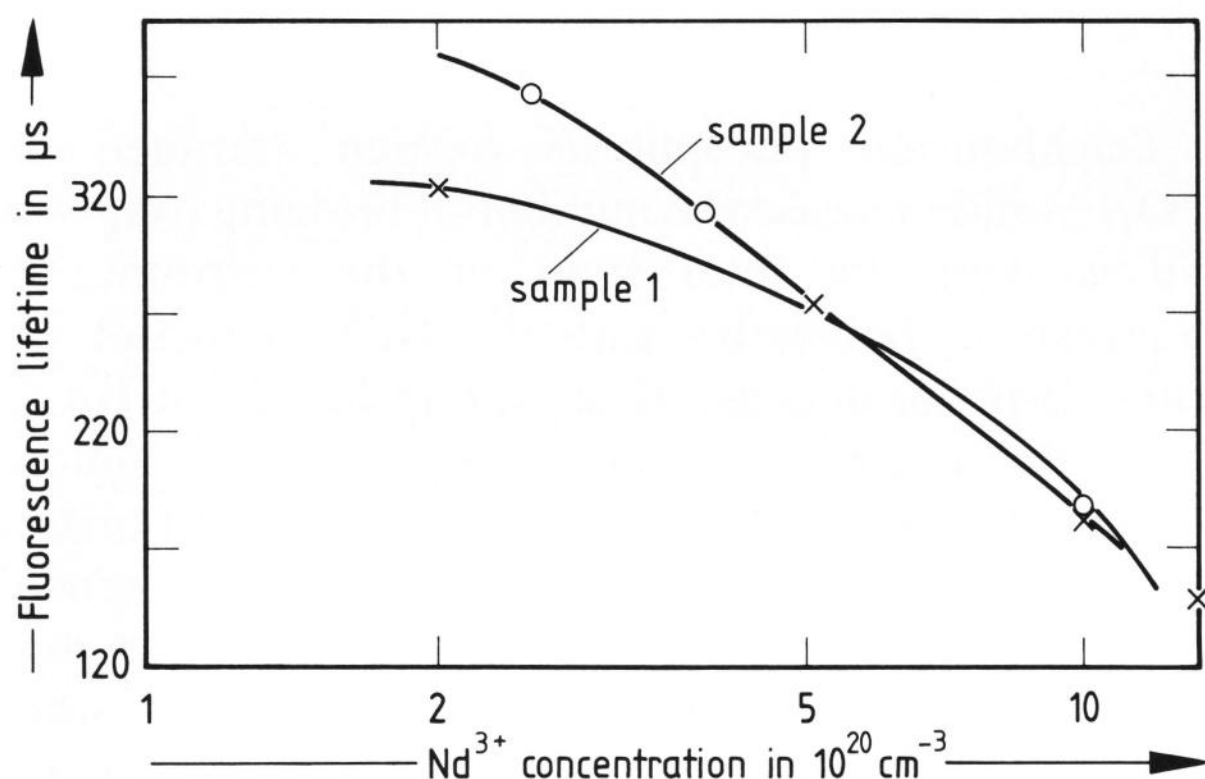


Figure 2. Comparison of Nd^{3+} quenching curves in two borophosphate glasses. The compositions (in mol%) of the samples 1 and 2 are as follows: 1 (corresponds to no. 59 in table 1): 66 P_2O_5 , 10 B_2O_3 , 6 Ln_2O_3 (= $La_2O_3 + Nd_2O_3$), 18 K_2O ; 2: 68.1 P_2O_5 , 11.8 Al_2O_3 , 6 Ln_2O_3 , 14.1 K_2O [4].

aluminium. While it is close to the two types of glass when the Nd^{3+} content is higher than $5 \cdot 10^{20}$ ions/cm³, for the fluorescence lifetime is dominated by the interaction between pairs of Nd^{3+} ions in high Nd^{3+} -doped glass. Figure 2 shows that the concentration quenching is weak in borophosphate glasses.

3.4. Thermal expansion coefficient and thermal shock resistance

The transformation temperature, T_g , the softening temperature, T_f , the thermal expansion coefficient, α , over a temperature interval from 25 to 100 °C, the calculated Young's modulus, E , the Poisson ratio, μ , the thermal conductivity, κ , and the ratio $\kappa(1-\mu)/\alpha E$ (FOM' = Figure of Merit) are presented in table 3 [14].

The combination of trivalent boron and pentavalent phosphorus in the tetrahedral coordination turns the structure of borophosphate glass into a structure resembling that of fused SiO_2 . The structure of phosphate glass is fortified by B_2O_3 , this is illustrated by table 3 in which the thermal expansion coefficient is very sensitive to change in boric content. It can be seen from table 3 that there is a close

relationship between the thermal expansion coefficient and the bonding strength between cations and oxygen.

It is well known that the thermal shock resistance of isotropic materials can be evaluated using the formula [15]:

$$FOM = \frac{S \kappa (1 - \mu)}{\alpha E} \quad (2)$$

where S is the tensile fracture strength. The tensile fracture strength is not a totally intrinsic property but depends on the physical condition of the surface of the material, and it is difficult to obtain precise values of the strength. Thus, the ratio $FOM' = \frac{\kappa(1-\mu)}{\alpha E}$

is usually used as the figure of merit for the thermal shock resistance. The larger the ratio FOM', the greater must be the thermal shock resistance. It is believed from the result that the borophosphate glass with high boric oxide content which has a low thermal expansion coefficient and a high value of the FOM' would have an improved thermal shock resistance.

4. Conclusions

a) The Nd^{3+} -doped borophosphate glass is possessed of a large stimulated emission cross-section, which increases with increasing B_2O_3 content. The effective linewidth of fluorescence depends on the B_2O_3 content and the bonding strength between cations and oxygen.

b) The influence of B_2O_3 , RO, and MO on fluorescence lifetimes is not significant in borophosphate glasses. The quantum efficiency of borophosphate glasses is large.

c) The thermal expansion coefficient decreases with increasing boron content and the bonding strength between cations and oxygen. The glass with high boron oxide content would have an improved thermal shock resistance.

d) It is believed that a Nd^{3+} -containing borophosphate glass with a stimulated emission cross-section of

$3.8 \cdot 10^{-20} \text{ cm}^2$, a fluorescence lifetime, τ_f , of $180 \mu\text{s}$ at $1 \cdot 10^{21} \text{ Nd}^{3+} \text{ ions/cm}^3$, a quantum efficiency of 0.50 and a thermal expansion coefficient of $85 \cdot 10^{-7} \text{ K}^{-1}$ could be obtained.

5. References

- [1] Coleman, L. W.; Storm, E.: Recent experiments in inertial confinement fusion. *Physics Today* **40** (1987) no. 1, p. s59–s61.
- [2] Bodner, S. E.: Recent progress in laser fusion. *Physics Today* **41** (1988) no. 1, p. s65–s67.
- [3] Hecht, J.: Laser fusion advance at LLNL and Rochester. *Laser Optronics* (1988) no. 5, p. 24–27.
- [4] Cook, L. M.; Marker III, A. J.; Stokowski, S. E.: Compositional effects on Nd^{3+} concentration quenching in the system $\text{R}_2\text{O} \cdot \text{Al}_2\text{O}_3 \cdot \text{Ln}_2\text{O}_3 \cdot \text{P}_2\text{O}_5$. *Proc. SPIE* **505** (1984) p. 102–111.
- [5] Stokowski, S. E.: Glasses for high power lasers. Lawrence Livermore National Laboratory Laser Program Annual Report. 1987. p. 9.57–59. Rep. UCRL-50021-86.
- [6] Hayden, J. S.; Sapak, D. L. et al.: Advances in glasses for high average power laser systems. *SPIE* **1021** (1988) p. 36–41.
- [7] Hoffmann, H. J.; Hayden, J. S.: Glasses as active materials for high average power solid state lasers. *SPIE* **1021** (1988) p. 42–50.
- [8] Jiang, Y.; Jiang, S.; Jiang, Y.: Spectral properties of Nd^{3+} in aluminophosphate glasses. *J. Non-Cryst. Solids* **112** (1989) p. 286–290.
- [9] Nasu, H.; Mackenzie, J. D.: Nonlinear optical properties of glasses and glass or gel-based composites. *Opt. Eng.* **26** (1987) no. 2, p. 102–106.
- [10] Krupke, W. F.: Induced-emission cross sections in neodymium laser glasses. *IEEE J. Quantum Electron.* **QE-10** (1974) p. 450–457.
- [11] Kravchenko, V. B.; Rudnitskii, J. P.: Phosphate laser glasses – Review. *Sov. J. Quantum Electron* **9** (1979) no. 4, p. 399–415.
- [12] Weber, M. J.; Saroyan, R. A.; Ropp, R. C.: Optical properties of Nd^{3+} in metaphosphate glasses. *J. Non-Cryst. Solids* **44** (1981) p. 137–148.
- [13] Izumitani, T.: Basic research for new laser glasses. *Rev. Laser Eng.* **3** (1974) p. 28–34.
- [14] Gan Fuxi: *Optical glasses*. (Orig. Chin.), Beijing: Science Publ. 1982.
- [15] Emmett, J. L.; Krupke, W. F.; Trenholme, J. B.: Future development of high power solid state laser systems. *Sov. J. Quantum Electron.* **13** (1983) p. 1–23.

91R1008